Available online at www.sciencedirect.com

ScienceDirect

Nuclear Physics A 1016 (2021) 122310

NUCLEAR PHYSICS A

www.elsevier.com/locate/nuclphysa

The activation cross section measurements of proton-induced reactions on Li and Ta in the energy region 12.5–34 MeV

Eva Šimečková [a], Mitja Majerle [a,*], Milan Štefánik [a], Jaromír Mrázek [a], Jan Novák [a], Tomáš Magna [b]

[a] *Nuclear Physics Institute of the CAS, 250 68 Řež near Prague, Czech Republic*
[b] *Czech Geological Survey, Klárov 3, CZ-118 21 Prague 1, Czech Republic*

Received 20 May 2021; received in revised form 1 September 2021; accepted 2 September 2021
Available online 1 October 2021

Abstract

The experimental data on cross sections are necessary to clarify existing ideas on the mechanisms of nuclear reactions and for testing of nuclear models. Proton-induced reaction on ^{7}Li serves as a source of quasi-monoenergetic neutrons which are widely used in the measurement of cross sections for neutron induced reactions. Tantalum plays an important role in technology and nuclear facilities mainly for its low induced activity (screens, degraders). In order to investigate the important nuclides, we have carried out the irradiation experiments with the variable-energy cyclotron U-120M of the NPI CAS Řež. The cross section of the reaction ^{7}Li(p,n)^{7}Be(ground state+0.43 MeV) and the cross sections of the nuclides ^{180,178m}Ta, ^{178}W and ^{175}Hf from reactions on natural tantalum were investigated, of which ^{181}Ta(p,n)^{180g}Ta for the first time. The stacked-foil technique was utilized. The comparison of new results with prior data and predictions of evaluations is discussed.

Keywords: Activation cross sections; Proton-induced reaction

* Corresponding author.
E-mail address: majerle@ujf.cas.cz (M. Majerle).

https://doi.org/10.1016/j.nuclphysa.2021.122310
0375-9474/

1. Introduction

Reaction p+^{7}Li is widely used as a source of quasi-monoenergetic (QM) neutrons at intermediate energies (ca. 20-50 MeV). The measurements with QM neutrons serve for the validation and measurement of reaction cross sections for various materials figuring in the design of new concepts of energy production (fusion, accelerator-driven systems). The reduction of uncertainties of the experimental data is crucial for the reliable functioning of these devices. Detailed knowledge of the neutron spectrum is therefore necessary for these measurements.

The QM neutron spectrum consists of a monoenergetic peak originating from the (p,n) reaction leading to the production of ^{7}Be (in the ground state and in the first excited state, 0+0.429 MeV) and low energy part (three body interactions leading to the decay of ^{7}Be) [22]. In the forward direction, approximately half of the produced neutrons in the spectrum belongs to peak neutrons. The data on ^{7}Be production together with the information about the angular distribution of peak neutrons [25] is used for absolute normalization of the produced neutron spectra.

The characteristics of the reaction ^{7}Li(p,n)^{7}Be(ground state+0.43 MeV) and produced peak neutrons have been studied in several works [16]. Existing experimental data for the ^{7}Be production in the energy interval of 10-40 MeV differ mutually by several percents and a dedicated measurement was performed to provide a new set of the experimental data.

We measured the cross sections of ^{7}Li(p,n)^{7}Be reaction in the energy region of 12.5-34 MeV. The irradiations were performed using the stacked-foil technique. The production of ^{7}Be was measured by the activation method. We took advantage of the fact that the tantalum foils were used for the energy reduction at irradiation runs and the cross sections of Ta(p,x) reactions were also determined. Tantalum is widely used in nuclear facilities for its small induced radioactivity, mechanical properties, resistance to corrosion, high melting point, and good thermal and electric conductivity. The irradiations were carried out at the CANAM infrastructure of the NPI CAS using the external proton beam of the variable-energy cyclotron U-120M operating in the negative-ion mode.

2. Experiment

2.1. Experimental setup

The proton irradiations of the stack of Li foils (interleaved with Ta degraders and Cu monitor foils) were performed using the U-120M cyclotron. The experimental setup used as QM neutron generator [15] was modified to accommodate the stack of foils about 3 cm thick followed by 1 cm thick carbon beam stop. This setup part (Faraday cup) was insulated from the rest of the generator and cooled by alcohol. The deposited proton charge was collected in the Faraday cup using ORTEC 439 Charge Integrator (Fig. 1).

Three different stacks were irradiated during independent runs with different initial energy (Table 1).

In the first run (E_p=34.41 MeV), four ^{nat}Li foils (Novosibirsk Chemical Concentrates Plant product, year 2000, declared thickness of 550 μm, corresponding to 29.4 mg/cm^2) were interleaved by ^{nat}Cu foils (25 μm declared thickness, purity 99.9%, Goodfellow product – CU 000 371) serving as monitors of the proton flux and energy, and ^{nat}Ta foils (50 μm declared thickness, purity 99.9%, Goodfellow product – TA 000 360) serving as proton energy degraders. The diam-

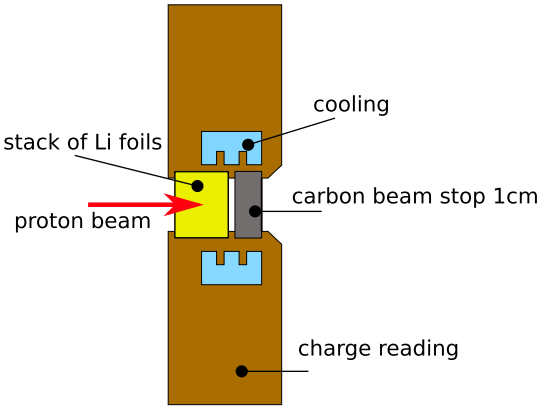

Fig. 1. Schematic drawing of the experimental setup – Faraday cup - where the stack of foils was inserted.

Table 1
Characteristics of individual runs.

E_p (MeV)	Li composition	Duration (s)	Q (μC)	I_{mean} (μA)
34.41	92.67% of ^{7}Li	2860.9	282.04	0.0986
25.08	pure ^{7}Li	2963.9	300.21	0.101
19.16	pure ^{7}Li	2310.0	251.87	0.109

eter of all foils in the stack was 15 mm. The ^{nat}Cu foils and ^{nat}Ta foils were precisely weighed to reduce the mass uncertainty declared by producer.

In the following two runs (E_p=25.08 MeV and E_p=19.16 MeV), enriched ^{7}Li foils were used (Sigma-Aldrich product, 2018, ≈500 μm thick disks produced by CAMEX Měšice). Lithium disks were weighed in the digester with argon atmosphere during the preparation of the stack. The weighing turned out to be sensitive to operational conditions of the digester; the individual weights were therefore averaged resulting in the average Li foil thickness of 26.7 mg/cm^2. The rest of the stack in the second run (E_p=25.08 MeV) was identical to the stack used in the first run, while in the third run (E_p=19.16 MeV) the proton energy degraders (^{nat}Ta foils) were not used.

The isotopic composition of ^{nat}Li and ^{7}Li foils was checked using a Neptune multiple-collector inductively-coupled-plasma mass spectrometer (MC-ICP-MS), housed at the Czech Geological Survey. The methodology is described in detail in [14]. The atomic ratio of ^{7}Li/^{6}Li in the sample of ^{nat}Li from the first run was measured at 12.641±0.009 (cf. natural Li with ^{7}Li/^{6}Li of 12.111±0.015, as measured for international reference material L-SVEC). The sample used in the first run has therefore ≈4.3% more ^{7}Li and the resulting percentage of 92.67% was used in the data analysis. In ^{7}Li-enriched samples used in the following two runs, no ^{6}Li was detected above the detection limit (estimated to concentration of 10 appm); it was thus considered as pure ^{7}Li.

The irradiations were performed with the proton beam extracted from the cyclotron U-120M operating in the negative-ion acceleration mode. The absolute accuracy of the proton beam energy is in the range of 100-200 keV [12], the proton energy distribution can be described by the gaussian distribution with the FWHM width of ≈200 keV. The proton beam was collimated

Table 2
Uncertainty budget of the measured cross sections.

Source of uncertainty	1^{st} run 34.41 MeV	2^{nd} run, 25.08 MeV	3^{rd} run, 18.48 MeV
Peak area - S	0.5-5%	0.5-5%	0.5-5%
n_{Li-7}/n_{Ta-181}	10%/<1%	10%/<1%	10%/<1%
$\epsilon_P(E)$	2%	2%	2%
Charge measurement - Φ	2-3%	2-3%	2-3%

and the stack was exposed to a relatively small average current of protons (100 nA) to avoid the melting of the Li foils. The irradiations lasted for 40-50 min (Table 1).

After the irradiations, the stack of foils was disassembled and the γ-ray spectra emitted from the individual foils were measured by two calibrated HPGe detectors of 50% efficiency at various detector to sample distance. The Li foils were stored in kerosene to avoid their degradation due to oxygen.

2.2. Data analysis

The γ-ray spectra measured with the HPGe detectors were analyzed using standard spectroscopic software and areas under γ peaks (S) were extracted. Standard spectroscopic formula was used to calculate the number of the produced nuclei of isotope A during irradiation as:

$$N(\mathrm{A}) = \frac{S \cdot \lambda \cdot t_{\mathrm{irr}}}{\epsilon_P(E) \cdot I_\gamma(E)} \frac{C_t}{\mathrm{COI} \cdot C_g \cdot C_s} \frac{t_{\mathrm{real}}}{t_{\mathrm{live}}} \frac{t_{\mathrm{irr}} \cdot e^{\lambda t_0}}{(1 - e^{-\lambda t_{\mathrm{irr}}})(1 - e^{-\lambda t_{\mathrm{real}}})}, \tag{1}$$

where λ is the decay constant ($\lambda = \frac{\ln(2)}{t_{1/2}}$), t_{irr} is the duration of the irradiation, t_{real} and t_{live} are the real and live acquisition times of the HPGe measurement and t_0 is the time interval from the end of the irradiation and the beginning of the HPGe measurement. The peak efficiency of the HPGe for γ photons of energy E is denoted by $\epsilon_P(E)$, $I_\gamma(E)$ is the γ-emission probability. Half-lives ($t_{1/2}$), the energies of the γ-ray transitions and their intensities were taken from the ENSDF database [23,17,1,3,19]. The correction for the decay cascade effect (COI) and the geometrical correction (C_g) were negligible for our measurements (large detector to sample distance was used), the corrections for the beam instabilities during the irradiation (C_t) and for the self-absorption of γ photons in the sample material (C_s) were considered.

The cross section is calculated from $N(\mathrm{A})$ as:

$$\sigma(E_p) = \frac{N(\mathrm{A})}{\Phi \cdot N_{\mathrm{tar}}}, \tag{2}$$

where Φ is the integral flux of protons and N_{tar} is the number of target atoms per surface unit. The energy E_p is calculated as the average proton energy in the specific sample by simulating the stack of the foils using the SRIM-2008 code [27].

The uncertainty budget of the resulting cross sections is shown in Table 2. The only significant contributions arise from the statistical uncertainty of the peak fitting procedure (0.5-5%, not correlated), uncertainties of the number of target nuclei in the foil (1-10%, strong correlation, for Li no correlation between 1^{st} and $2^{nd}/3^{rd}$ runs), peak efficiency calibration of the HPGe (2%, strong correlation), and charge measurement (2-3%, strong correlation).

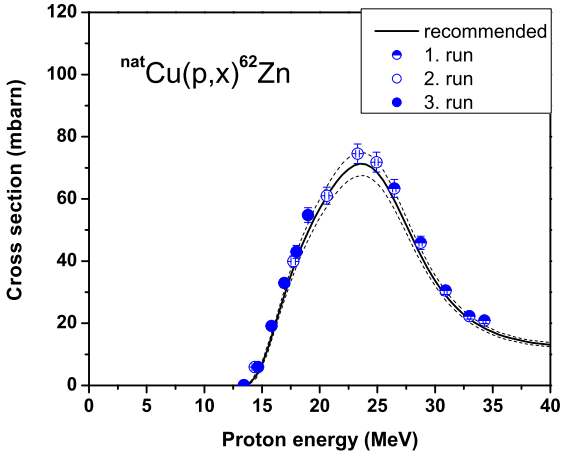

Fig. 2. ^{nat}Cu(p,x)^{62}Zn cross section (values are tabulated in Table 3). Present results are compared to charged particle reference cross section [8].

Table 3
The cross section of the ^{nat}Cu(p,x)^{62}Zn monitor reaction.

E_p(MeV)	σ (mbarn)
13.42(24)	0.14(1)
14.37(23)	5.91(27)
14.67(23)	5.95(26)
15.83(22)	19.1(83)
16.93(20)	33.0(15)
17.70(20)	39.9(17)
17.98(20)	43.0(20)
18.98(19)	54.8(24)
20.62(18)	61.0(27)
23.28(16)	74.5(31)
24.92(15)	71.8(32)
26.46(15)	63.4(29)
28.75(14)	45.9(21)
30.92(13)	30.6(13)
32.97(12)	22.3(9)
34.29(12)	20.9(10)

3. Results

In all three runs, the stack of measured samples was interleaved with the ^{nat}Cu monitor foils. The obtained experimental cross sections of the reaction ^{nat}Cu(p,x)^{62}Zn ($t_{1/2}$=9.193min, E_γ=596.56/548.35 keV, I_γ=26/15.34%) were compared with the recommended excitation functions for this reaction [8]. From the comparison in Fig. 2, it is apparent that all three runs are in agreement with the reference cross sections - within the uncertainty limits. However, a small systematic shift of the experimental results to greater values (in comparison with the reference curve) is obvious - on average ≈3%. The absolute energy of the proton beam and the deposited charge were therefore under control.

Table 4
The cross section of the ^{7}Li(p,n)^{7}Be reaction.

E_p(MeV)	σ (mbarn)
12.76(42)	47.3(51)
14.05(39)	44.0(47)
15.25(36)	40.2(43)
16.09(35)	36.8(39)
16.39(34)	36.1(38)
17.46(32)	37.9(41)
18.48(31)	35.4(38)
19.19(30)	32.4(35)
21.98(27)	30.5(33)
24.52(25)	25.0(27)
27.62(24)	26.8(29)
29.85(23)	24.3(27)
31.96(22)	22.6(24)
33.96(21)	21.7(23)

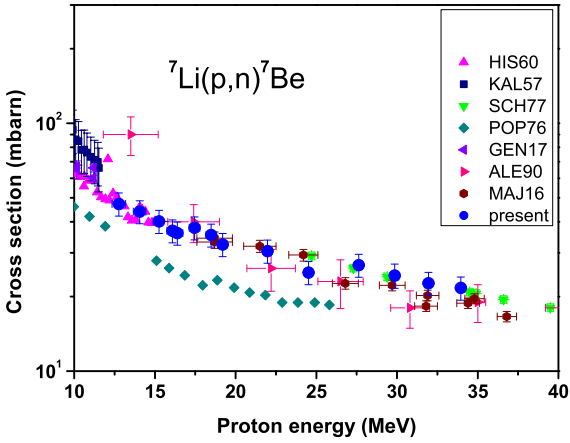

Fig. 3. ^{7}Li(p,n)^{7}Be cross section. Present values compared with data of other authors in the energy region 10-40 MeV. (For interpretation of the colors in the figure(s), the reader is referred to the web version of this article.)

3.1. p+^{7}Li

The γ-ray spectroscopy was used to obtain the number of produced nuclei of ^{7}Be ($t_{1/2}$ = 53.22 d, E_γ=477.6035 keV, I_γ=10.44%). The data obtained from ^{nat}Li irradiation were normalized to the natural abundance of ^{7}Li in the sample as the contribution of ^{7}Be production from the reaction ^{6}Li(p,γ)^{7}Be reaction is negligible.

The resulting cross sections are shown in Table 4 and Fig. 3 together with the published data. Our new results are in satisfactory agreement with our preceding results [15], and with data published elsewhere [9,10,21,6]. The data from [2] with larger uncertainties disagree with our new and other experimental data sets. The cross-section data from [20], which are also in disagreement with other data sets, were not obtained using γ-ray spectrometry but instead, they

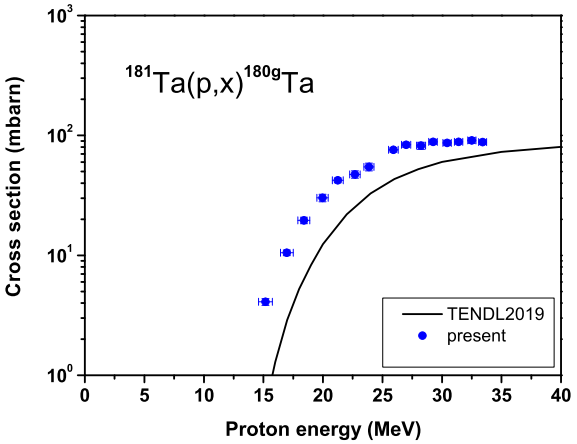

Fig. 4. ^{181}Ta(p,x)^{180g}Ta cross section.

were calculated from the integral of the measured differential peak neutron cross sections and normalized to the absolute measurement from [7].

3.2. p+^{181}Ta

Natural Ta consists of two isotopes [18]: ^{181}Ta (99.988%) and ^{180m}Ta (0.012%) isomeric state with the half-live of $> 4.5 \cdot 10^{16}$y [13]. The contributions of the reactions induced on ^{180m}Ta to the measured cross sections are below the uncertainties of the results and are thus considered negligible. The results are therefore presented as the cross sections for the ^{181}Ta isotope.

The measured cross sections of the ^{181}Ta(p,x)^{180g}Ta reaction are shown in Fig. 4. The ^{180g}Ta decays with the half-life of 8.154h through 103.6 keV (0.864%) γ-ray transitions. Because of strong background contribution around 93 keV, only the γ-ray line with the energy of 103.6 keV was taken into account for the cross section determination. The experimental cross-section values, determined for the first time in this study, are in a broad agreement with the theoretical excitation curve of TENDL-2019 evaluation [11]. The contribution to the production of ^{180g}Ta from the decay of the isomeric state was several orders of magnitude below the production by the ^{181}Ta(p,x)^{180g}Ta reaction (10^{-2}Bq against $\approx 10^5$ Bq).

The reaction ^{181}Ta(p,*)^{178}Ta produces ^{178g}Ta and ^{178m}Ta isomers. The isomer ^{178g}Ta with the half-life of 9.31 m could not be measured (too long interval between the end of the irradiation and the start of the measurements). For ^{178m}Ta, the only allowed decay mode from this isomeric state is the direct decay to ^{178}Hf emitting 426.355 keV (97.4%) and 325.555 keV (94.1%) γ-rays ($t_{1/2}$=2.36h). The resulting cross sections are shown in Fig. 5. Present data are in agreement with TENDL-2019 evaluation and with other experimental data [5].

Isotope ^{178}W produced by the reaction ^{181}Ta(p,4n)^{178}W decays (by electron capture) to the ^{178g}Ta isomeric state emitting only X-rays (Q=91.3(20)keV, $t_{1/2}$=21.6d). Single X-ray transition of 57.535 keV (13.9%) is suitable for ^{178}W activity determination (blue circle). The subsequent decay of ^{178g}Ta to ^{178}Hf with $t_{1/2}$=9.31min (E_γ=1350.55/1340.85 keV, I_γ=1.176/1.0272%) was also used to determine the ^{178}W activity. The amount of ^{178g}Ta produced during the irradiation by the reaction ^{181}Ta(p,*)^{178g}Ta decays quickly and after more than 2 hours of cooling time one can suppose that the state ^{178g}Ta is fully fed solely from the decay of ^{178}W (^{178m}Ta is also produced

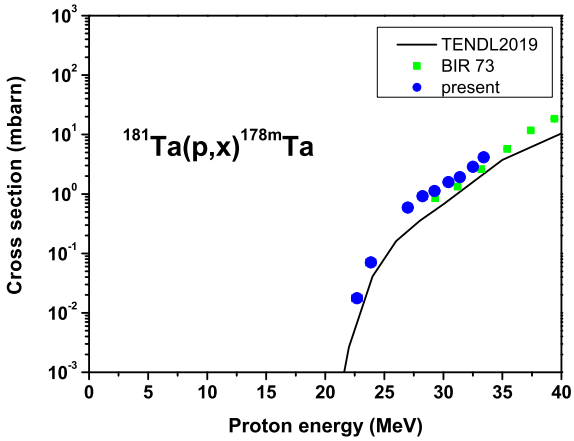

Fig. 5. ^{181}Ta(p,x)^{178m}Ta cross section. Present values are compared to the TENDL-2019 evaluation [11] and to other experimental data [5].

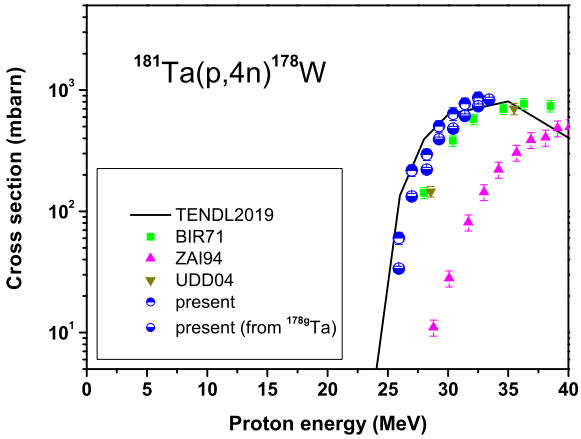

Fig. 6. ^{181}Ta(p,4n)^{178}W cross section. Present values are compared to the TENDL-2019 evaluation [11] and to other experimental data [4,24,26].

but does not decay through ^{178g}Ta). Both sets of new data are in agreement with TENDL-2019 evaluation and with results of [4] and [24]. Data from [26] appears to be shifted in energy (Fig. 6).

The cross sections of the reaction ^{181}Ta(p,x)^{175}Hf were determined using the γ-ray transition 343.4 keV (84%), $t_{1/2}$=70d. The results are shown in Fig. 7.

The new experimental cross section for all measured reactions on Ta are presented numerically in Table 5.

4. Conclusion

The cross sections for ^{7}Li(p,n)^{7}Be reaction were measured in the energy range of 12.5-34 MeV. The new experimental data are in agreement with the majority of the previous results and, in addition, provide a single set of the experimental data in the entire energy range. Tantalum foils were used for proton energy degraders and were activated during irradiations. With the analysis

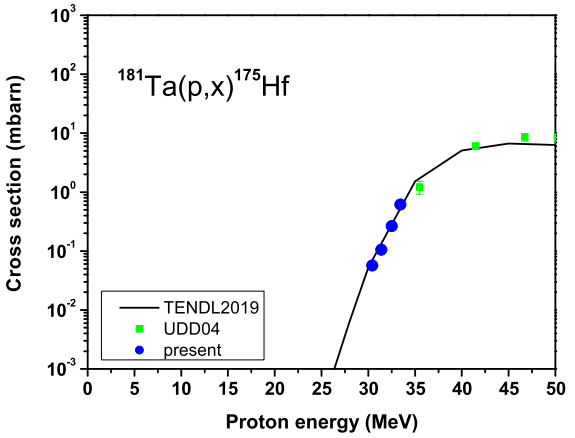

Fig. 7. ^{181}Ta(p,x)^{175}Hf cross section. Present values are compared to the TENDL-2019 evaluation [11] and to other experimental data [24].

Table 5
Cross sections for isotopes produced in Ta foils. Data marked by (*) are determined from the secondary decay of ^{178m}Ta, because the measured activities of 57.535 keV γ-ray transition (from ^{178}W decay) are burdened by the error from the extrapolation of the efficiency curve towards small energies.

E_p(MeV)	σ(^{180g}Ta)	σ(^{178}W)*	σ(^{178m}Ta)	σ(^{175}Hf)
15.17(58)	4.09(26)			
16.97(54)	10.5(57)			
18.40(50)	19.6(12)			
19.97(47)	30.2(21)			
21.25(46)	42.2(20)			
22.68(44)	47.4(33)		0.018(2)	
23.86(42)	54.7(40)		0.070(4)	
25.91(40)	75.9(32)	33.7(14)		
26.99(39)	83.7(40)	133(8)	0.59(4)	
28.24(38)	82.2(56)	221(9)	0.92(12)	
29.25(36)	88.4(42)	394(17)	1.12(7)	
30.43(35)	86.7(42)	481(20)	1.59(9)	0.057(6)
31.39(35)	88.5(37)	611(26)	1.92(8)	0.105(7)
32.51(34)	90.9(50)	735(34)	2.86(12)	0.266(24)
33.42(33)	87.9(37)	838(35)	4.15(27)	0.615(48)

of the tantalum foils, the cross sections for four different reactions of ^{181}Ta with protons were determined. The cross sections for the reaction ^{181}Ta(p,x)^{180g}Ta were experimentally measured for the first time. Present values are in agreement with the TENDL-2019 evaluation and with majority of other earlier presented data.

CRediT authorship contribution statement

Eva Šimečková: Methodology. **Mitja Majerle:** Conceptualization. **Milan Štefánik:** Visualization. **Jaromír Mrázek:** Supervision. **Jan Novák:** Software. **Tomáš Magna:** Methodology.

All authors contributed to writing of the manuscript.

Declaration of competing interest

The authors declare that they have no known competing financial interests or personal relationships that could have appeared to influence the work reported in this paper.

Acknowledgements

The measurements were carried out at the infrastructure CANAM of the NPI CAS Řež, supported by The Ministry of Education, Youth and Sports of the Czech Republic under the project EF16_013/0001812. TM contributed through the Strategic Research Plan of the Czech Geological Survey (DKRVO/ČGS 2018-2022).

References

[1] E. Achterberg, O. Capurro, G. Marti, Nuclear data sheets for A = 178, Nucl. Data Sheets 110 (7) (2009) 1473–1688, https://doi.org/10.1016/j.nds.2009.05.002.

[2] V. Aleksandrov, M.P. Semenova, V.G. Semenov, The production of Be-7 at middle energy protons interaction with light nuclei, Vopr. Atomn. Nauki i Tekhn., Ser. Yad. Fiz. Issledo. (8/16) (1990) 17.

[3] M.S. Basunia, Nuclear data sheets for A = 175, Nucl. Data Sheets 102 (4) (2004) 719–900, https://doi.org/10.1016/j.nds.2004.09.002.

[4] C. Birattari, E. Gadioli, A. Strini, G. Strini, G. Tagliaferri, L. Zetta, (p, xn) reactions induced in 169Tm, 181Ta and 209Bi with 20 to 45 MeV protons, Nucl. Phys. A 166 (3) (1971) 605–623, https://doi.org/10.1016/0375-9474(71)90909-2.

[5] C. Birattari, E. Gadioli, A.M. Grassi Strini, G. Strini, G. Tagliaferri, Interpretation of nucleon emission from the bombardment of 181Ta with protons, Lettere Nuovo Cimento (1971–1985) 7 (3) (May 1973) 101–107, https://doi.org/10.1007/BF02727609.

[6] L.N. Generalov, S.N. Abramovich, S.M. Selyankina, Bull. Russ. Acad. Sci., Phys. 81 (6) (Jun 2017) 644–657, https://doi.org/10.3103/S1062873817060107.

[7] J.H. Gibbons, R.L. Macklin, Total neutron yields from light elements under proton and alpha bombardment, Phys. Rev. 114 (Apr 1959) 571–580, https://doi.org/10.1103/PhysRev.114.571.

[8] A. Hermanne, A. Ignatyuk, R. Capote, B. Carlson, J. Engle, M. Kellett, T. Kibédi, G. Kim, F. Kondev, M. Hussain, O. Lebeda, A. Luca, Y. Nagai, H. Naik, A. Nichols, F. Nortier, S. Suryanarayana, S. Takács, F. Tárkányi, M. Verpelli, Reference cross sections for charged-particle monitor reactions, in: Special Issue on Nuclear Reaction Data, Nucl. Data Sheets 148 (2018) 338–382, https://doi.org/10.1016/j.nds.2018.02.009.

[9] K. Hisatake, Y. Ishizaki, A. Isoya, T. Nakamura, Y. Nakano, B. Saheki, Y. Saji, K. Yuasa, The reactions Li7(p, n)Be7, B11(p, n)C11 and Al27(p, n)Si27 at 8 to 14 MeV, J. Phys. Soc. Jpn. 15 (5) (1960) 741–748, https://doi.org/10.1143/JPSJ.15.741.

[10] S.P. Kalinin, A.A. Ogloblin, Y.M. Petrov, Excitation functions for the reactions Li7(p. n)Be7, B10(p.α)Be7, and B11(p. n)C11, and energy levels in Be8, C11, and C12 nuclei, Sov. J. At. Energy 2 (2) (Mar 1957) 193–196, https://doi.org/10.1007/BF01832091.

[11] A. Koning, D. Rochman, J.-C. Sublet, N. Dzysiuk, M. Fleming, S. van der Marck TENDL, Complete nuclear data library for innovative nuclear science and technology, in: Special Issue on Nuclear Reaction Data, Nucl. Data Sheets 155 (2019) 1–55, https://doi.org/10.1016/j.nds.2019.01.002.

[12] A. Morgenstern, O. Lebeda, J. Stursa, F. Bruchertseifer, R. Capote, J. McGinley, G. Rasmussen, M. Sin, B. Zielinska, C. Apostolidis, Production of 230U/226Th for targeted alpha therapy via proton irradiation of 231Pa, Anal. Chem. 80 (22) (2008) 8763–8770, https://doi.org/10.1021/ac801304c.

[13] B. Lehnert, M. Hult, G. Lutter, K. Zuber, Search for the decay of nature's rarest isotope ^{180m}Ta, Phys. Rev. C 95 (Apr 2017) 044306, https://doi.org/10.1103/PhysRevC.95.044306.

[14] T. Magna, U. Wiechert, A. Halliday, Low-blank isotope ratio measurement of small samples of lithium using multiple-collector ICPMS, Int. J. Mass Spectrom. 239 (2004) 67–76, https://doi.org/10.1016/j.ijms.2004.09.008.

[15] M. Majerle, P. Bém, J. Novák, E. Šimečková, M. Štefánik, Au, Bi, Co and Nb cross-section measured by quasimonoenergetic neutrons from p + ^{7}Li reaction in the energy range of 18-36 MeV, Nucl. Phys. A 953 (2016) 139–157, https://doi.org/10.1016/j.nuclphysa.2016.04.036.

[16] M. Majerle, A.V. Prokofiev, M. Ansorge, P. Bém, D. Hladík, J. Mrázek, J. Novák, E. Simecková, M. Stefánik, Peak neutron production from the ^{7}Li(p,n) reaction in the 20-35 MeV range, EPJ Web Conf. 239 (2020) 20010, https://doi.org/10.1051/epjconf/202023920010.

[17] E. McCutchan, Nuclear data sheets for A = 180, Nucl. Data Sheets 126 (2015) 151–372, https://doi.org/10.1016/j.nds.2015.05.002.

[18] J. Meija, T.B. Coplen, M. Berglund, W.A. Brand, P.D. Bièvre, M. Gröning, N.E. Holden, J. Irrgeher, R.D. Loss, T. Walczyk, T. Prohaska, Isotopic compositions of the elements 2013 (IUPAC Technical Report), Pure Appl. Chem. 88 (3) (2016) 293–306, https://doi.org/10.1515/pac-2015-0503.

[19] A.L. Nichols, B. Singh, J.K. Tuli, Nuclear data sheets for A = 62, Nucl. Data Sheets 113 (4) (2012) 973–1114, https://doi.org/10.1016/j.nds.2012.04.002.

[20] C.H. Poppe, et al., Cross sections for the ^{7}Li$(p,n)^{7}$Be reaction between 4.2 and 26 MeV, Phys. Rev. C 14 (Aug 1976) 438–445, https://doi.org/10.1103/PhysRevC.14.438.

[21] S. Schery, L. Young, R. Doering, S.M. Austin, R. Bhowmik, Activation and angular distribution measurements of ^{7}Li(p, n)^{7}Be(0.0+0.49 MeV) for Ep=25-45 MeV: a technique for absolute neutron yield determination, Nucl. Instrum. Methods 147 (2) (1977) 399–404, https://doi.org/10.1016/0029-554X(77)90275-0.

[22] M. Takada, T. Nakamura, M. Baba, T. Iwasaki, T. Kiyosumi, Characterization of 22 and 33 MeV quasi-monoenergetic neutron fields for detector calibration at CYRIC, Nucl. Instrum. Methods Phys. Res., Sect. A, Accel. Spectrom. Detect. Assoc. Equip. 372 (1) (1996) 253–261, https://doi.org/10.1016/0168-9002(95)01247-8.

[23] D. Tilley, C. Cheves, J. Godwin, G. Hale, H. Hofmann, J. Kelley, C. Sheu, H. Weller, Energy levels of light nuclei A=5, 6, 7, Nucl. Phys. A 708 (1) (2002) 3–163, https://doi.org/10.1016/S0375-9474(02)00597-3.

[24] M. Uddin, M. Hagiwara, N. Kawata, T. Itoga, N. Hirabayashi, M. Baba, F. Tarkanyi, F. Ditroi, J. Csikai, Measurement of excitation functions of the proton-induced activation reactions on tantalum in the energy range 28-70 MeV, J. Nucl. Sci. Technol. 41 (sup4) (2004) 160–163, https://doi.org/10.1080/00223131.2004.10875669, https://www.tandfonline.com/doi/pdf/10.1080/00223131.2004.10875669.

[25] Y. Uwamino, T.S. Soewarsono, H. Sugita, Y. Uno, T. Nakamura, T. Shibata, M. Imamura, S. Shibata, High-energy p-Li neutron field for activation experiment, Nucl. Instrum. Methods Phys. Res., Sect. A, Accel. Spectrom. Detect. Assoc. Equip. 389 (3) (1997) 463–473, https://doi.org/10.1016/S0168-9002(97)00345-8.

[26] N.G. Zaitseva, E. Rurarz, V.A. Khalkin, V.I. Stegailov, L.M. Popinenkova, Excitation function for ^{178}W production in the ^{181}Ta(p, 4n)^{178}W reaction over proton energy range 28.8-71.8 MeV, Radiochim. Acta 64 (1) (1994) 1–6, https://doi.org/10.1524/ract.1994.64.1.1.

[27] J.F. Ziegler, J.P. Biersack, SRIM-2008, Stopping power and range of ions in matter, http://inis.iaea.org/search/search.aspx?orig_q=RN:40107606, May 2008, MATHEMATICAL METHODS AND COMPUTING.